Structural and first magnetic characterization of unique mono-μ-chloro bridged dinuclear Cu^{II} complexes with heterocycle-functionalized diazamesocyclic ligands

Miao Du,[a] Ya-Mei Guo,[a] Xian-He Bu,*[a] Joan Ribas[b] and Montserrat Monfort[b]

[a] *Department of Chemistry, Nankai University, Tianjin 300071, P. R. China. E-mail: buxh@nankai.edu.cn; Fax: +86-22-23502458*

[b] *Departament de Química Inorgànica, Universitat de Barcelona, Diagonal 647, 08028 Barcelona, Spain*

Received (in London, UK) 25th February 2002, Accepted 15th March 2002
First published as an Advance Article on the web 5th June 2002

Two new diazamesocyclic ligands based on 1,4-diazacycloheptane (DACH), functionalized by additional heterocyclic donor groups, 1,4-bis(pyridin-2-ylmethyl)-1,4-diazacycloheptane (L^1) and 1,4-bis(imidazol-4-ylmethyl)-1,4-diazacycloheptane (L^2), together with their Cu^{II} complexes $[Cu_2(\mu\text{-}Cl)(L^1)_2](ClO_4)_3$ (**1**) and $[Cu_2(\mu\text{-}Cl)(L^2)_2](ClO_4)_3$ (**2**), have been synthesized and characterized. Single crystal X-ray diffraction analyses revealed that both complexes have the unique mono-μ-Cl dimeric $[Cu_2(\mu\text{-}Cl)(L)_2]^{3+}$ structural motif. For both complexes, each Cu^{II} center is penta-coordinate in a distorted square-pyramidal environment with the bridging chloride atom at the apical position. The magnetic properties of mono-μ-chloro Cu^{II} dinuclear complexes have been investigated for the first time through the study of complexes **1** and **2** by variable temperature magnetic susceptibility and magnetization measurements. Weak ferromagnetic (for **1**) or anti-ferromagnetic (for **2**) interactions between the two Cu^{II} centers have been found and possible magneto-structural correlations have been analyzed.

Introduction

Particular interest has been directed towards the investigation of dinuclear Cu^{II} complexes in order to elucidate the spin coupling between paramagnetic metal centers, both from structural and theoretical points of view,[1–3] especially for the monatomically bridged (*e.g.* μ-OH, OCH_3, S and Cl) Cu^{II} dimers,[4,5] since they provide the simplest case of magnetic interaction involving only two unpaired electrons. Concurrent with this has been the development of the magneto-structural correlation in the $[Cu(\mu\text{-}Cl)_2Cu]$ dimeric motif with two chloride bridges, which displays a wealth of structures with a variety of Cu–Cl lengths and Cu–Cl–Cu angles, depending on the coordinated ligands and also on the counterions.[6,7] In contrast, Cu^{II} complexes exhibiting only one chloride bridge are quite scarce, and almost all of these compounds have the one-dimensional linear structure, with the chloride bridge placed at the equatorial-axial positions in the chain.[8] To the best of our knowledge, only two isolated dinuclear Cu^{II} complexes with only one chloride bridge have been reported, but without magnetic studies;[9] additionally, very few examples of Cu^{II} complexes with one chloride bridging ligand and other different bridging ligand(s) have been investigated and magnetically characterized so far.[10]

In our efforts[11] to systematically investigate the control of the structures and magnetic properties, as well as the coordination chemistry of diazamesocyclic ligands,[12] predominantly for 1,5-diazacyclooctane (DACO), we have reported a variety of Cu^{II} complexes with different coordination modes and magnetic properties by altering the donor pendants on them. One of the main reasons for the continuing interest in this attractive system is the ability to construct other novel metal complexes with special topologies and properties by modification of the diazamesocycle backbone; by choosing 1,4-diazacycloheptane (DACH) as the initial material, for example. In this contribution, we report the syntheses and characterization of two new heterocycle-functionlized diazamesocyclic ligands, 1,4-bis(pyridin-2-ylmethyl)-1,4-DACH (L^1) and 1,4-bis(imidazol-4-ylmethyl)-1,4-DACH (L^2) (Chart 1). It is interesting that two unique mono-μ-Cl bridged dimeric compounds $[Cu_2(\mu\text{-}Cl)(L^1)_2](ClO_4)_3$ (**1**) and $[Cu_2(\mu\text{-}Cl)(L^2)_2](ClO_4)_3$ (**2**) were obtained by the reaction of L^1 or L^2 with Cu^{II}, with structures which are quite different from the mononuclear structures of the Cu^{II} complexes[11] obtained with the corresponding heterocycle-functionlized 1,5-diazacyclooctane ligands, indicating that the nature of the backbone of the diazamesocycle is a determining factor governing the structure and properties of the Cu^{II} complexes. Furthermore, the magnetic coupling properties of such complexes are reported for the first time herein and possible magneto-structural correlations are discussed in detail.

Experimental

Materials and general methods

Most of the starting materials, such as 1,4-diazacycloheptane (DACH) and 2-chloromethylpyridine hydrochloride, and solvents for syntheses were obtained commercially and used as received. 4-Chloromethylimidazole hydrochloride was pre-

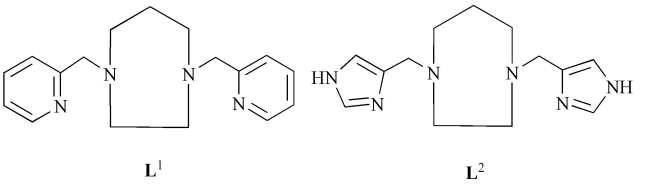

L^1 L^2

Chart 1

DOI: 10.1039/b201962k

pared according to the literature method.[13] FT-IR spectra (KBr pellets) were taken on a FT-IR 170SX (Nicolet) spectrometer and electronic absorption spectra on a Hitachi UV-3010 spectrometer. Carbon, hydrogen and nitrogen analyses were performed on a Perkin–Elmer 240C analyzer. ^{1}H NMR spectra were recorded on a Bruker AC-P 400 spectrometer (400 MHz) at 25 °C with tetramethylsilane as the internal reference. EPR spectra were recorded on powder samples at X-band frequency with a BRUKER 300E automatic spectrometer, varying the temperature between 4 and 300 K.

Syntheses of ligands

1,4-Bis(pyridin-2-ylmethyl)-1,4-diazacycloheptane trihydrochloride tetrahydrate (L^1·3HCl·4H_2O). 2-Chloromethylpyridine hydrochloride (3.07 g, 18.3 mmol) was added to a solution of DACH (0.87 g, 8.7 mmol) in C_2H_5OH (50 mL) with vigorous stirring at room temperature. Small portions of solid KOH were added to the mixture to ensure that the pH value stayed at 8–9 for *ca.* 2 days. After filtration of the mixture, the solvent was removed by rotary evaporation. The residue was purified by silica gel column chromatography (CH_2Cl_2:CH_3OH:NH_3·H_2O = 10:10:1), and the free ligand oil was further purified by conversion to its HCl salt, which was obtained as a white crystalline solid. Yield: 2.26 g (55% based on DACH). ^{1}H NMR (D_2O): δ 2.14–2.19 (m, 2H), 3.36 (t, J = 5.4 Hz, 4H), 3.52 (s, 4H), 4.51 (s, 4H), 7.82 (t, J = 6.6 Hz, 2H), 7.88 (d, J = 7.6 Hz, 2H), 8.33 (t, J = 7.4 Hz, 2H), 8.71 (d, J = 5.2 Hz, 2H). IR (KBr pellet, cm^{-1}): 3345b, 2956m, 2613s, 2170w, 1642s, 1617s, 1545m, 1479m, 1463s, 1432m, 1387m, 1108m, 1018m, 947m, 921m, 785s, 773m. Anal. calcd for $C_{17}H_{22}N_4$·3HCl·4H_2O: C, 44.02; H, 7.17; N, 12.08%. Found: C, 43.81; H, 7.29; N, 11.72%.

1,4-Bis(imidazol-4-ylmethyl)-1,4-diazacycloheptane pentahydrochloride hydrate (L^2·5HCl·H_2O). To a solution of DACH (0.38 g, 3.7 mmol) in CH_3OH (50 mL) was added 4-chloromethylimidazole hydrochloride (1.23 g, 8.0 mmol) with vigorous stirring. Small portions of solid KOH were added to keep the pH value of the mixture at *ca.* 9. After 3 days of stirring, the mixture was filtered and the solvent was removed by rotary evaporation. Then, the residue was purified by silica gel column chromatography (CH_2Cl_2:CH_3OH:NH_3·H_2O = 5:5:1), and the free ligand was further purified by conversion to its HCl salt, which was obtained as a white solid. Yield: 0.94 g (55% based on DACH). ^{1}H NMR (D_2O): δ 2.34 (t, J = 3.2 Hz, 2H), 3.61 (t, J = 5.2 Hz, 4H), 3.88 (d, J = 3.6 Hz, 4H), 4.68 (t, J = 4.4 Hz, 4H), 7.84 (s, 2H), 8.86 (t, J = 1.8 Hz, 2H). IR (KBr pellet, cm^{-1}): 3354b, 2985b, 1624s, 1529w, 1478s, 1457s, 1433vs, 1405s, 1367m, 1319m, 1273m, 1256w, 1168m, 1111m, 1079s, 1014m, 939m, 916s, 902m, 828s, 771m, 626s. Anal. calcd for $C_{13}H_{20}N_6$·5HCl·H_2O: C, 33.89; H, 5.91; N, 18.25%. Found: C, 33.79; H, 6.17; N, 18.13%.

Syntheses of Cu^{II} complexes

[Cu_2(μ-Cl)(L^1)$_2$](ClO_4)$_3$ (1). Complex **1** was prepared by mixing equimolar amounts of L^1·3HCl·4H_2O (47 mg, 0.1 mmol) and $Cu(ClO_4)_2$·6H_2O (37 mg, 0.1 mmol) in methanol (25 mL). The pH value of this solution was adjusted to *ca.* 6–7 with dilute aqueous KOH solution. After *ca.* 30 min of stirring, the blue solution was filtered and left to stand at room temperature. Block-like blue single crystals suitable for X-ray analysis were obtained by slow evaporation of the solvent. Yield: 36 mg (70%). IR (KBr pellet, cm^{-1}): 2930m, 1611s, 1573w, 1485m, 1463m, 1450s, 1438s, 1302m, 1162s, 1090vs, 1039s, 1024m, 985m, 768s, 623vs. Anal. calcd for $C_{34}H_{44}Cl_4Cu_2N_8O_{12}$: C, 39.82; H, 4.32; N, 10.93%. Found: C, 39.77; H, 4.58; N, 10.81%.

[Cu_2(μ-Cl)(L^2)$_2$](ClO_4)$_3$ (2). Complex **2** was synthesized similarly in 75% yield. IR (KBr pellet, cm^{-1}): 2914m, 1624m, 1593m, 1506m, 1481m, 1467s, 1446m, 1379m, 1346m, 1269s, 1144vs, 1116vs, 1088vs, 1024vs, 1011s, 636s, 625vs. Anal. calcd for $C_{26}H_{36}Cl_4Cu_2N_{12}O_{12}$: C, 31.94; H, 3.71; N, 17.20%. Found: C, 31.72; H, 4.01; N, 16.98%.

Caution! Although no problems were encountered in this study, transition metal perchlorate complexes are potentially explosive and should be handled with appropriate precautions.

Magnetic studies

The variable temperature magnetic susceptibilities were measured at the "Servei de Magnetoquímica" (Universitat de Barcelona) on polycrystalline samples (30 mg) with a Quantum Design MPMS SQUID susceptometer operating at a magnetic field of 0.1 T between 2 and 300 K. Diamagnetic corrections were evaluated from Pascal's constants for all the constituent atoms. Magnetization measurements were carried out at 2 K in the 0–5 T range.

X-Ray diffraction

Single crystal X-ray diffraction studies were performed on a Bruker Smart 1000 CCD diffractometer equipped with a graphite crystal monochromator situated in the incident beam for data collection. The determination of unit cell parameters and data collections were performed with Mo-Kα radiation (λ = 0.71073 Å). The structures were solved by direct methods and semi-emperical absorption corrections were applied using the SADABS program. Cu^{II} atoms in each complex were located from the *E*-maps and the other non-hydrogen atoms were located in successive difference Fourier syntheses. The final refinement was performed by full-matrix least-squares methods with anisotropic thermal parameters for non-hydrogen atoms on F^2. Hydrogen atoms were generated theoretically onto the atoms to which they are attached and refined isotropically with fixed thermal factors. Further details of the structural analyses are summarized in Table 1.

CCDC reference numbers 181896 and 181897. See http://www.rsc.org/suppdata/nj/b2/b201926k/ for crystallographic data in CIF or other electronic format.

Results and discussion

Syntheses and general characterization

Both new doubly substituted ligands L^1 and L^2 were prepared by using an excess of the hydrochloride of 2-chloromethylpyridine or 4-chloromethylimidazole, and purified by silica gel column chromatography. Acid-free ligands were obtained as oils so that they were converted into the HCl salts to get further purified crystalline solids. The yields for both ligands are over 50% and all the analytical data are in good agreement with the theoretical requirements.

The syntheses of the complexes were achieved by reaction of the acid-free ligand with Cu^{II}. Since the corresponding ligands are the HCl salts, they must be neutralized with KOH solution prior to complexation. The IR spectra for both complexes show absorption bands resulting from the skeletal vibrations of the aromatic rings in the 1400–1600 cm^{-1} region. The interesting features of the spectra for both complexes are the occurrence of highly split ν_{Cl-O} stretches due to the ClO_4^- ions at ~1100 cm^{-1}, which provides good evidence for their involvement in hydrogen bonding.

Description of crystal structures

[Cu_2(μ-Cl)(L^1)$_2$](ClO_4)$_3$ (1). An ORTEP view of the monochloro bridged dimeric [Cu_2(μ-Cl)(L^1)$_2$]$^{3+}$ cation in complex

Table 1 Summary of crystal data for $[Cu_2(\mu\text{-}Cl)(L^1)_2](ClO_4)_3$ (**1**) and $[Cu_2(\mu\text{-}Cl)(L^2)_2](ClO_4)_3$ (**2**)

	1	**2**
Formula	$C_{34}H_{44}Cl_4Cu_2N_8O_{12}$	$C_{26}H_{36}Cl_4Cu_2N_{12}O_{12}$
Fw	1025.65	977.55
Crystal system	Monoclinic	Orthorhombic
Space group	$P2_1/n$	$P2_12_12_1$
a/Å	14.571(4)	11.462(4)
b/Å	14.761(4)	12.790(4)
c/Å	19.596(5)	26.465(9)
β/°	90.235(5)	90
V/Å^3	4215.0(19)	3880(2)
Z	4	4
ρ_{calcd}/g cm^{-3}	1.616	1.674
μ/cm^{-1}	13.32	14.45
Reflns, unique/observed	7446/5000	6801/3181
R^a	0.0418	0.0578
$R_w{}^b$	0.1092	0.1110
Largest peak, hole/e Å^{-3}	0.640, 0.446	0.870, 0.518

^{a} $R = \Sigma||F_o| - |F_c||/\Sigma|F_o|$. ^{b} $R_w = [\Sigma[w(F_o{}^2 - F_c{}^2)^2]/\Sigma w(F_o{}^2)^2]^{1/2}$.

1, including the atomic numbering scheme, is given in Fig. 1. Both Cu^{II} centers are penta-coordinated (CuN_4Cl) to four nitrogen atoms of the diazamesocyclic ligand L^1, forming the basal planes, and the bridging chloride anion at the apical positions. The coordination polyhedron for Cu(1) can be best described as a square pyramid, which is reflected in the τ value (0.036 here) defined by Addison *et al.* ($\tau = 0$ for an ideal square pyramid, and 1 for an ideal trigonal bipyramid).[14] For Cu(2), the τ value is 0.45, indicating an intermediate state between an ideal square pyramid (SP) and a trigonal bipyramid (TBP). The Cu(1) atom is 0.262 Å above the mean basal plane defined by N(1)–N(2)–N(3)–N(4), toward the apical Cl(1), and for Cu(2), the corresponding value is 0.294 Å above the mean N(5)–N(6)–N(7)–N(8) plane. The Cu–Cl bond lengths [2.4911(13) and 2.4591(13) Å, see Table 2] are significantly shorter than those in the di-μ-Cl dinuclear motifs, which are normal in the 2.7–3.0 Å range,[4,5] and the Cu–Cl–Cu bridging angle is 149.50(6)°. The intramolecular Cu(1)···Cu(2) distance is 4.776(3) Å, significantly longer than those in the di-μ-Cl dinuclear complexes. The shortest intermolecular separations for Cu(1)···Cu(2)^i ($i = 0.5 + x,\ 0.5 - y,\ -0.5 + z$), Cu(1)···Cu(1)^i ($i = 2 - x,\ -y,\ -z$) and Cu(2)···Cu(2)^i ($i = 2 - x,\ 1 - y,\ 1 - z$) are 8.013(6), 8.565(4) and 8.226(4) Å, respectively.

In the ligand L^1, both DACH rings in $[Cu_2(\mu\text{-}Cl)(L^1)_2]^{3+}$ cation adopt the normal boat configuration. The dihedral angle between the pendant pyridine rings in the ligand bound to Cu(1) is 14.0(2)° and that for the other ligand bound to Cu(2) is 43.7(5)°. One feature of this structure is that each Cl(3)/O(5)/O(6)/O(7)/O(8) ClO_4^- counter anion links four different $[Cu_2(\mu\text{-}Cl)(L^1)_2]^{3+}$ cationic unit in a (η^3, μ^4) bridging mode [η^3: O(5), O(7) and O(8)] through intermolecular C–H···O interactions, which is reflected in the highly split ClO_4^- bands in the IR spectrum of **1**.

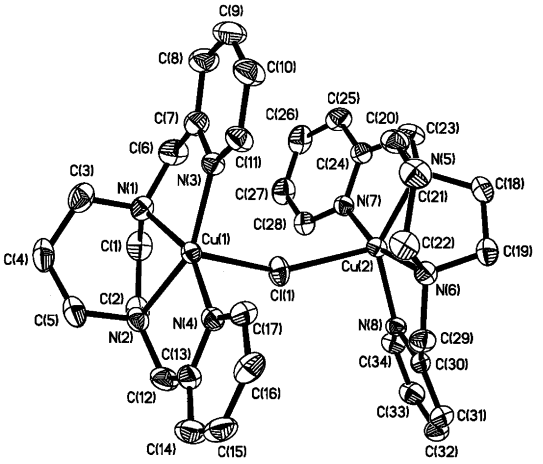

Fig. 1 ORTEP view of the dimeric $[Cu_2(\mu\text{-}Cl)(L^1)_2]^{3+}$ cationic unit of **1**, with 50% thermal probability ellipsoids.

$[Cu_2(\mu\text{-}Cl)(L^2)_2](ClO_4)_3$ (2). The crystal structure of **2** is similar to that of **1**, consisting of a mono-chloro bridged $[Cu_2(\mu\text{-}Cl)(L^2)_2]^{3+}$ dimeric cation (see Fig. 2) and three ClO_4^- ions. Both Cu^{II} centers are also penta-coordinated in distorted square-pyramidal geometry with the bridging chloride anion at the apical positions, having τ values of 0.028 for Cu(1) and 0.055 for Cu(2). Cu(1) is 0.267 Å above the mean N(1)–N(2)–N(3)–N(4) basal plane, toward the apical Cl(1), and Cu(2) is 0.232 Å above the N(7)–N(8)–N(9)–N(10) mean plane. The Cu–Cl bond lengths are 2.706(2) and 2.757(2) Å (see Table 3), significantly longer than those in **1**. The Cu–Cl–Cu bridging angle is 177.35(9)°, almost linear. The intramolecular Cu(1)···Cu(2) distance is 5.461(2) Å, significantly longer than that in **1**. The shortest intermolecular separations for Cu(1)···Cu(2)^i ($i = -0.5 + x,\ 0.5 - y,\ -0.5 - z$), Cu(1)···Cu(1)^i ($i = 1 - x,\ -0.5 + y,\ 0.5 - z$) and

Table 2 Selected bond distances (Å) and angles (°) for complex **1**

Cu(1)–N(1)	2.021(3)	Cu(1)–N(2)	2.022(3)
Cu(1)–N(4)	2.026(4)	Cu(1)–N(3)	2.034(3)
Cu(1)–Cl(1)	2.4911(13)	Cu(2)–N(7)	1.976(3)
Cu(2)–N(6)	2.001(3)	Cu(2)–N(5)	2.027(3)
Cu(2)–N(8)	2.043(3)	Cu(2)–Cl(1)	2.4591(13)
N(1)–Cu(1)–N(2)	78.28(15)	N(1)–Cu(1)–N(4)	158.46(14)
N(2)–Cu(1)–N(4)	83.46(14)	N(1)–Cu(1)–N(3)	82.57(14)
N(2)–Cu(1)–N(3)	156.32(14)	N(4)–Cu(1)–N(3)	111.75(14)
N(1)–Cu(1)–Cl(1)	97.08(11)	N(2)–Cu(1)–Cl(1)	97.88(11)
N(4)–Cu(1)–Cl(1)	96.64(10)	N(3)–Cu(1)–Cl(1)	98.19(10)
N(7)–Cu(2)–N(6)	164.88(14)	N(7)–Cu(2)–N(5)	84.94(14)
N(6)–Cu(2)–N(5)	79.98(14)	N(7)–Cu(2)–N(8)	107.42(14)
N(6)–Cu(2)–N(8)	83.41(14)	N(5)–Cu(2)–N(8)	138.09(14)
N(7)–Cu(2)–Cl(1)	91.56(10)	N(6)–Cu(2)–Cl(1)	97.64(11)
N(5)–Cu(2)–Cl(1)	123.04(11)	N(8)–Cu(2)–Cl(1)	97.08(9)
Cu(2)–Cl(1)–Cu(1)	149.50(6)		

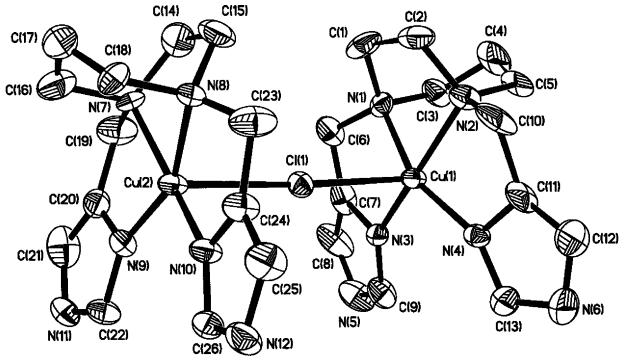

Fig. 2 ORTEP view of the dimeric $[Cu_2(\mu\text{-}Cl)(\mathbf{L}^2)_2]^{3+}$ cationic unit of **2**, with 50% thermal probability ellipsoids.

$Cu(2)\cdots Cu(2)^i$ $(i = -0.5 + x,\ 0.5 - y,\ -z)$ are 8.096(3), 8.785(2) and 7.775(2) Å, respectively.

Both DACH rings in **2** also adopt the normal boat configuration. The dihedral angle between the imidazole rings in the ligand bound to Cu(1) is 22.0(3)° and that for the other ligand bound to Cu(2) is 9.0(2)°. Similarly to **1**, there are also multiple inter- and intra-molecular C–H···O hydrogen bonds, reflected in the highly split ClO_4^- bands in the IR spectrum of **2**. It should be noted that **2** is in the chiral non-centric space group $P2_12_12_1$, with a Flack parameter of 0.03(3) (near zero), indicating that the absolute structure is correct.

Electronic and EPR spectra

The UV-Vis spectral data for complexes **1** and **2** (blue) in methanol solution show broad and intense absorption maxima centered at 634 and 588 nm, respectively. This spectral feature is typical of penta-coordinate Cu^{II} complexes with (distorted) square-pyramidal geometry, which generally exhibit a band in the 550–660 nm range ($d_{xz}, d_{yz} \rightarrow d_{x^2-y^2}$).[15] Complex **1** displays a higher λ_{max} than that of **2**, suggesting more distortion toward a trigonal bipyramid geometry,[16] which is consistent with the degree of distortion found in the X-ray structural analysis. In addition, the electronic spectra of both complexes display characteristic absorptions at 200–300 nm assigned to ligand $\pi \rightarrow \pi^*$ transitions.

The X-band EPR spectra of both complexes were aquired in the solid state at different temperatures (from room temperature to 4 K). For **1**, at all temperatures, the spectra do not show anisotropic features, only an isotropic band centered at $g_{av} = 2.08$, probably due to exchange narrowing. No absorption is observed at half-field ($\Delta m_s = 2$, $g = 4$), as might be expected for ferromagnetic coupling, and this feature also indicates a small zero-field splitting effect.[17] For **2**, at all temperatures, there is a pattern typical of axial distortion, with $g_{\|} = 2.17$, $g_{\perp} = 2.05$ and $g_{av} = 2.09$, and there is no variation with temperature. This pattern is typical for Cu^{II} complexes with square-pyramidal geometry, with the unpaired electron mainly located in the $d_{x^2-y^2}$ orbital.

Table 3 Selected bond distances (Å) and angles (°) for complex **2**

Cu(1)–N(4)	1.946(9)	Cu(1)–N(3)	1.958(9)
Cu(1)–N(2)	2.018(8)	Cu(1)–N(1)	2.034(9)
Cu(1)–Cl(1)	2.706(2)	Cl(1)–Cu(2)	2.757(2)
Cu(2)–N(9)	1.940(9)	Cu(2)–N(10)	1.944(8)
Cu(2)–N(7)	2.013(9)	Cu(2)–N(8)	2.018(8)
N(4)–Cu(1)–N(3)	106.5(3)	N(4)–Cu(1)–N(2)	85.7(4)
N(3)–Cu(1)–N(2)	158.0(4)	N(4)–Cu(1)–N(1)	159.7(4)
N(3)–Cu(1)–N(1)	85.2(4)	N(2)–Cu(1)–N(1)	78.3(4)
N(4)–Cu(1)–Cl(1)	97.8(3)	N(3)–Cu(1)–Cl(1)	95.6(3)
N(2)–Cu(1)–Cl(1)	100.7(3)	N(1)–Cu(1)–Cl(1)	97.4(2)
N(9)–Cu(2)–N(10)	108.0(3)	N(9)–Cu(2)–N(7)	85.0(4)
N(10)–Cu(2)–N(7)	161.1(4)	N(9)–Cu(2)–N(8)	157.8(4)
N(10)–Cu(2)–N(8)	86.2(4)	N(7)–Cu(2)–N(8)	77.5(4)
N(9)–Cu(2)–Cl(1)	95.4(3)	N(10)–Cu(2)–Cl(1)	96.9(3)
N(7)–Cu(2)–Cl(1)	95.3(3)	N(8)–Cu(2)–Cl(1)	99.8(3)
Cu(1)–Cl(1)–Cu(2)	177.35(9)		

Magnetic properties

The magnetic properties of complex **1**, in the form of χ_M and $\chi_M T$ *vs.* T plots, are shown in Fig. 3(a), where the the magnetic susceptibility is for two Cu^{II} ions. The χ_M values range from 0.00266 $cm^3\ mol^{-1}$ at 300 K to 0.51 $cm^3\ mol^{-1}$ at 2 K. The value of $\chi_M T$ at room temperature is 0.80 $cm^3\ mol^{-1}$ K. This value corresponds to two independent Cu^{II} ions without coupling, with $g > 2.0$. The $\chi_M T$ value increases monotonically up to 1.96 K, attaining a value of 1.00 $cm^3\ mol^{-1}$ K. This global feature is characteristic of the presence of weak ferromagnetic interactions between the Cu^{II} ions. A very good fit can be obtained through a simple Bleaney–Bowers expression for a Cu^{II} dimer,[18,19] giving the following parameters: $J = 2.25$ cm^{-1}, $g = 2.06$ and $R = 9 \times 10^{-6}$ {R is the agreement factor

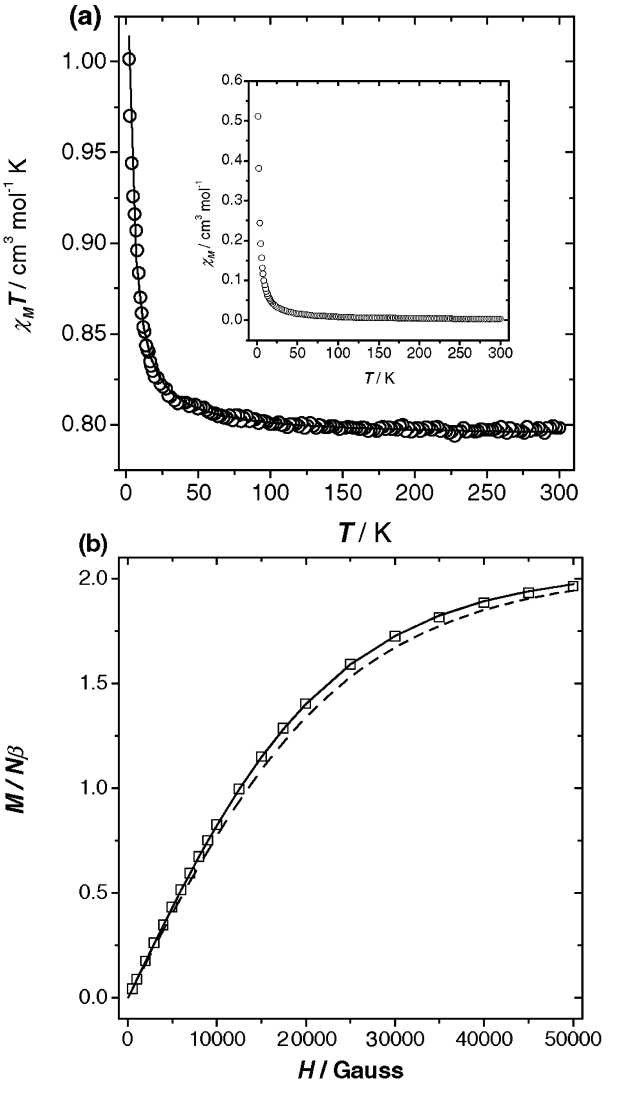

Fig. 3 Magnetic properties of **1**. (a) Temperature dependence of $\chi_M T$ and χ_M (insert). (b) Field dependence of the reduced magnetization at 2 K ($M/N\beta$, number of electrons per formula unit): (□) experimental points; (·····) Brillouin curve for isolated Cu^{II} ions; (——) best fit obtained (see text for calculated parameters).

defined as $\Sigma_i[(\chi_M T)_{obs} - (\chi_M T)_{calc}]^2/\Sigma[(\chi_M T)_{obs}]^2\}$. To corroborate the order of magnitude of this small ferromagnetic parameter, magnetization measurements were carried out at very low temperature (2 K). The reduced magnetization ($M/N\beta$) curve *vs.* H does not exactly follow the Brillouin law [Fig. 3(b)]. At intermediate fields, the experimental points are above the theoretical curve, indicating weak ferromagnetism. At 5 T the $M/N\beta$ value tends to 2.0, which corresponds to an $S = 1$ ground state (close to saturation). The experimental curve has been fit using a magnetic program (full-diagonalization method) valid for dinuclear systems.[20] A very good fit was obtained with the following parameters: $J = 2.06$ cm^{-1}, $g = 2.08$ and $R = 7.6 \times 10^{-6}$ (R is the agreement factor defined above). Fig. 3(b) shows the experimental data and the corresponding fit. The two J values (from susceptibility and magnetization measurements) are very similar, of the same order of magnitude: 2.25 and 2.06 cm^{-1}, respectively. In these systems with a small magnetic coupling (like **1** and **2**), the J values obtained from magnetization data are more accurate than those obtained from susceptibility data.

The magnetic properties of complex **2**, in the form of χ_M and $\chi_M T$ *vs.* T plots, are shown in Fig. 4(a), where the magnetic susceptibility is for two Cu^{II} ions. The χ_M values range from 0.00276 cm^3 mol^{-1} at 300 K to 0.30 cm^3 mol^{-1} at 2 K. The value of $\chi_M T$ at room temperature is 0.83 cm^3 mol^{-1} K, corresponding to two independent Cu^{II} ions without coupling ($g > 2.0$). The $\chi_M T$ value decreases monotonically to 1.95 K, attaining a value of 0.60 cm^3 mol^{-1} K. This curve shape is characteristic of the presence of weak antiferromagnetic interactions between the Cu^{II} ions. A very good fit can be obtained through a simple Bleaney–Bowers expression for a Cu^{II} dimer,[18,19] giving the following parameters: $J = -1.30$ cm^{-1}, $g = 2.10$ and $R = 2.1 \times 10^{-6}$. The coupling parameter is so small that no maximum in the χ_M curve is observed until 2 K. To corroborate the order of magnitude of this small antiferromagnetic parameter, magnetization measurements were also carried out at very low temperature (2 K). The reduced magnetization ($M/N\beta$) curve *vs.* H does not exactly follow the Brillouin law [Fig. 4(b)]. At intermediate fields, the experimental points are below the theoretical curve, indicating weak antiferromagnetism. At 5 T, the $M/N\beta$ value tends to 2.0, corresponding to an $S = 1$ ground state (close to the saturation). The experimental curve was also been fit with the program mentioned above.[20] A very good fit was obtained with the following parameters: $J = -1.12$ cm^{-1}, $g = 2.07$ and $R = 5.4 \times 10^{-6}$. Fig. 4(b) shows the experimental data and the corresponding fit. The two J values (from susceptibility and magnetization measurements) are very similar, of the same order of magnitude: -1.30 and -1.12 cm^{-1}.

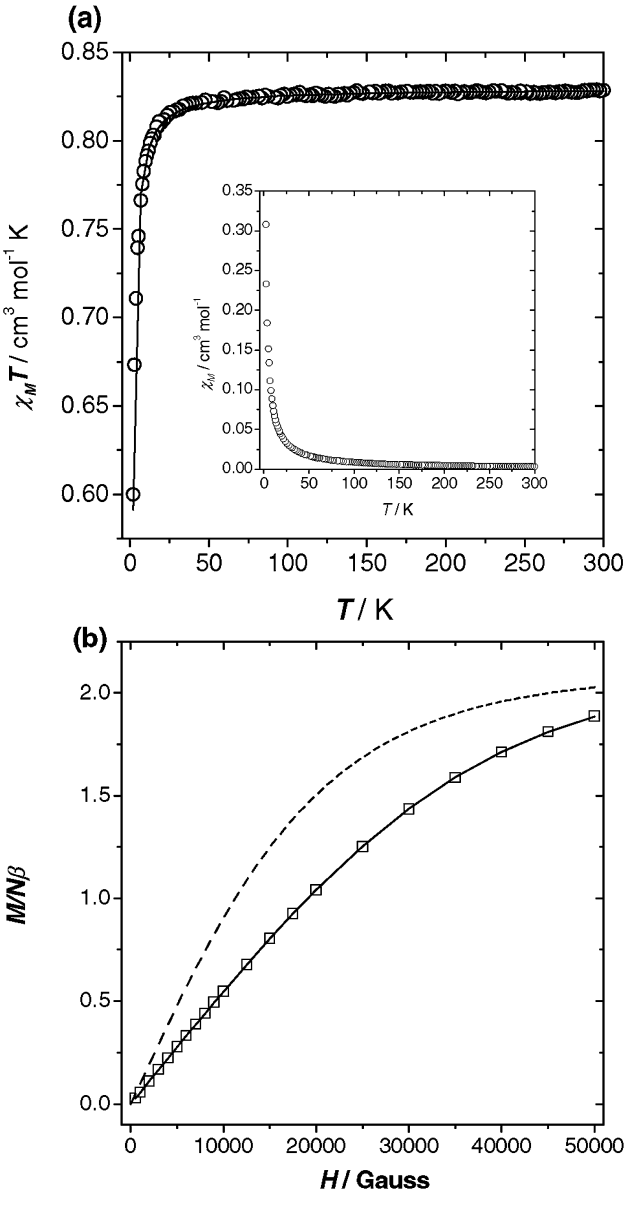

Fig. 4 Magnetic properties of **2**. (a) Temperature dependence of $\chi_M T$ and χ_M (insert). (b) Field dependence of the reduced magnetization at 2 K ($M/N\beta$, number of electrons per formula unit): (□) experimental points; (·····) Brillouin curve for isolated Cu^{II} ions; (——) best fit obtained (see text for calculated parameters).

Magneto-structural correlations

In almost all the mono-chloride bridged Cu^{II} complexes reported so far, the Cu^{II} ions show distorted square-pyramidal geometry, and the cases in which the coordination polyhedron of Cu^{II} is trigonal bipyramidal or octahedral are quite rare.[21] Assuming square-pyramidal geometry for Cu^{II}, as in **1** and **2**, there are three reported coordination modes for the chloride bridge: equatorial–equatorial (type I); equatorial–axial (apical) (type II) and axial (apical)–axial (apical) (type III) (Scheme 1). Type I is extremely rare and the few cases known contain another bridging ligand.[22] Type II is the most frequent in one-dimensional structures, with the chloride bridge placed equatorial–axial in the chain.[8] The two compounds studied in this work belong to the system with the chloride bridge in the axial–axial (or apical–apical) position (type III), as noted in the discussion of the structures.

As indicated above, only two Cu^{II} dimers show this kind of isolated monochloro bridging ligands, but the magnetic properties have not been studied. For mono-chloro bridged Cu^{II}

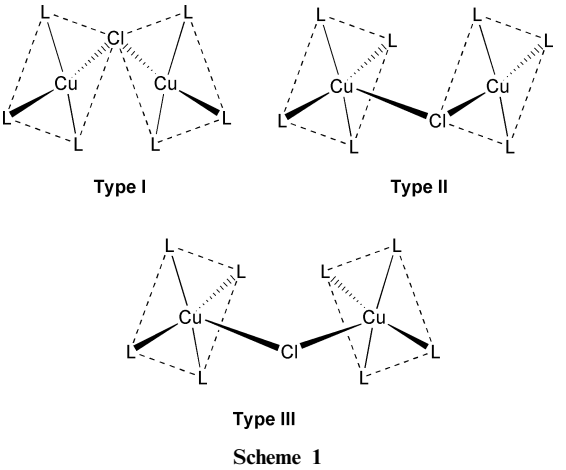

Scheme 1

Table 4 Comparison of the main structural data and magnetic parameters for apical–apical mono-μ-Cl Cu^{II} complexes {Im = imidazole; hatth = 3,6,9,17,20,23-hexaazatricyclo[23.3.1.1^{11,13}]triaconta-1(29),11(30),12,14, 25(26),27-hexaene; bpym = bipyrimide; ox = oxalato}

Complex	d_{Cu-N}[a]/Å	d_{Cu-Cl}/Å	$\theta_{Cu-Cl-Cu}$/°	τ	J/cm^{-1}	Ref.
$[Cu_2(\mu\text{-}Cl)(\mathbf{L}^1)_2](ClO_4)_3$	2.02	2.46, 2.49	149.50	0.45, 0.04	2.25	This work
$[Cu_2(\mu\text{-}Cl)(\mathbf{L}^2)_2](ClO_4)_3$	1.99	2.75, 2.71	177.35	0.06, 0.03	−1.30	This work
$[(hatth)_2Cu_4(Im)_2Cl_2]^{4+}$	2.05	2.55, 2.57	169.1	0.33, 0.27	−9.52	10(*a*)
$[Cu_2(bpym)(ox)Cl_2]_n$	2.00	2.56, 2.84	124.1	—	+8(2)[b]	10(*b*)

[a] Average value. [b] The authors use the Hamiltonian $\boldsymbol{H} = -2J\Sigma\mathbf{S}_i\mathbf{S}_j$, thus we give half the value indicated in the paper (+16 cm^{-1}) to correlate with our values. On the other hand, this value was calculated from the mean-field model. According to the authors, "It could be subject to question."

complexes, no magneto-structural correlations have been reported so far. The structural and magnetic data for the two other known complexes with monochloro bridging ligands and another different bridge(s), together with those for complexes **1** and **2**, are gathered in Table 4. In all cases, the chloride ion occupies the axial positions, where the spin density of the unpaired electron is expected to be low. Due to the possibility of structural distortion from square-pyramidal to trigonal bipyramidal coordination, there could be mixing of the Cu^{II} $d_{x^2-y^2}$ orbital with the d_{z^2} orbital. Thus, the unpaired electron density on the Cu^{II} ions, which is mainly in the $d_{x^2-y^2}$ orbital, may also be dispersed into the d_{z^2} orbital. In complex **1**, the τ parameters are 0.45 and 0.04, and in **2**, they are 0.06 and 0.03, respectively. Thus, one of the two Cu^{II} ions in **1**, and both Cu^{II} ions in **2**, are almost perfectly square-pyramidal in geometry, with no significant electron density in the apical d_{z^2} orbital. It might be expected, therefore, that there would be very small ferromagnetic coupling in both **1** and **2**. On the other hand, the size of the Cu–Cl–Cu angles may play a significant role in the coupling: for **1**, the Cu–Cl–Cu angle is close to 150°, whereas for **2**, it is close to 180°. The linearity introduces an antiferromagnetic coupling factor because the possible electron density in d_{z^2} overlaps perfectly with the p_z orbital of the chloride bridge. As a result of the near-linear orbital overlap between the Cu^{II} centers and the bridging chloride, an antiferromagnetic exchange interaction can be expected for linear complexes. The longer Cu–Cl bond distances in this case (2.71 and 2.76 Å) mitigate against appreciable antiferromagnetic coupling. In **1**, the Cu–Cl bond lengths are shorter (2.46 and 2.49 Å) and, together with the non-linearity of the Cu–Cl–Cu angle, result in a small ferromagnetic coupling.

Conclusion

In summary, two unique mono-μ-Cl bridged Cu^{II} dimers with new diazamesocyclic ligands functionalized by heterocyclic pendants have been rationally designed and synthesized, and the interesting coordination modes of Cu^{II} with such ligands have been elucidated by X-ray analyses. The magnetic coupling properties of such complexes have been investigated for the first time. As stated in ref. 10(*a*), "Copper complexes with a monochloride ion bridge which mediates the exchange interaction are very few and there is no magneto-structural correlation developed". In any event, since small changes in the coordination geometry are associated with profound changes in the coupling exchange, no final conclusions can be drawn from our work and the limit literature values. More examples of complexes like **1** and **2** are needed in order to further explore this meaningful magneto-structural correlation. Furthermore, the Cu^{II} ions in both complexes have weakly coordinated axial chloride anions, which may be replaced by other donor molecules or ions (such as azide, thiocyanate, cyanate, *etc*.) to form the corresponding Cu^{II} dimers. This work is currently under way in our laboratory.

Acknowledgements

This work was financially supported by the NSF of China (no. 29971019) and the Spanish government (grant BQU2000–0791).

References and notes

1 See for examples: (*a*) *Magneto-Structural Correlations in Exchange Coupled Systems*, ed. R. D. Willett, D. Gatteschi and O. Kahn, NATO ASI Ser. no. 140, D. Reidel, Dordrecht, 1984; (*b*) O. Kahn, Y. Pei and Y. Journaux, in *Inorganic Materials*, ed. Q. W. Bruce and D. O'Hare, John Wiley & Sons, Chichester, 1992; (*c*) D. Gatteschi, O. Kahn, J. S. Miller and F. Palacio, *Magnetic Molecular Materials*, Kluwer Academic, Dordrecht, 1991.

2 See for examples: (*a*) I. Castro, M. L. Calatayud, J. Sletten, F. Lloret, J. Cano, M. Julve, G. Seitz and K. Mann, *Inorg. Chem.*, 1999, **38**, 4680; (*b*) O. Kahn *Acc. Chem. Res.*, 2000, **33**, 647; (*c*) G. Psomas, C. P. Raptopoulou, L. Iordanidis, C. Dendrinou-Samara, V. Tangoulis and D. P. Kessissoglou, *Inorg. Chem.*, 2000, **39**, 3042; (*d*) I. Fernandez, R. Ruiz, J. Faus, M. Julve, F. Lloret, J. Cano, X. Ottenwaelder, Y. Journaux and M. C. Munoz, *Angew. Chem., Int. Ed.*, 2001, **40**, 3039.

3 See for examples: (*a*) A. Asokan, B. Varghese and T. Manoharan, *Inorg. Chem.*, 1999, **38**, 4393; (*b*) F. F. De. Biani, E. Ruiz, J. Cano, J. J. Novoa and S. Alvarez, *Inorg. Chem.*, 2000, **39**, 3221; (*c*) R. E. D. Sesto, A. M. Arif and J. S. Miller, *Inorg. Chem.*, 2000, **39**, 4894; (*d*) C. Blanchet-Boiteux and J.-M. Mouesca, *J. Am. Chem. Soc.*, 2000, **122**, 861.

4 See for examples: (*a*) G. De. Munno, M. Julve, F. Lloret, J. Cano and A. Caneschi, *Inorg. Chem.*, 1995, **34**, 2048; (*b*) K. Geetha, M. Nethaji, A. R. Chakravarty and N. Y. Vasanthacharya, *Inorg. Chem.*, 1996, **35**, 7666; (*c*) J. Ruiz, P. Alemany, S. Alvarez and J. Cano, *J. Am. Chem. Soc.*, 1997, **119**, 1297; (*d*) L. K. Thompson, S. S. Tandon, F. Lloret, J. Cano and M. Julve, *Inorg. Chem.*, 1997, **36**, 3301.

5 See for examples: (*a*) L. K. Thompson, S. K. Mandel, S. S. Tandon, J. N. Brisdon and M. K. Park, *Inorg. Chem.*, 1996, **35**, 3117; (*b*) B. Cervera, R. Ruiz, F. Lloret, M. Julve, J. Cano, J. Faus, C. Bois and J. Mrozinski, *J. Chem. Soc., Dalton Trans.*, 1997, 395; (*c*) E. Ruiz, P. Alemany, S. Alvarez and J. Cano, *Inorg. Chem.*, 1997, **36**, 3683; (*d*) W. Plass, A. Pohlmann and J. Rautengarten, *Angew. Chem., Int. Ed.*, 2001, **40**, 4207.

6 (*a*) S. S. Roberts, D. R. Bloomquist, R. D. Willett and H. W. Dodgen, *J. Am. Chem. Soc.*, 1981, **103**, 2603; (*b*) W. E. Marsh, W. E. Hatfield and D. J. Hodgson, *Inorg. Chem.*, 1982, **21**, 2679; (*c*) W. E. Marsh, K. C. Patel, D. J. Hodgson and W. E. Hatfield, *Inorg. Chem.*, 1983, **22**, 511; (*d*) D. K. Town, S. K. Hoffmann, W. E. Hatfield, P. Singh, P. Chaudhuri and K. Wieghardt, *Inorg. Chem.*, 1985, **24**, 4393; (*e*) C. P. Landee and R. E. Greeney, *Inorg. Chem.*, 1986, **25**, 3371.

7 (*a*) T. Rojo, M. I. Arriortua, J. Ruiz, J. Darriet, J. Villeneuve and D. Beltran-Porter, *J. Chem. Soc., Dalton Trans.*, 1987, 285; (*b*) P. Baran, M. Koman, D. Valigura and J. Mrozinski, *J. Chem. Soc., Dalton Trans.*, 1991, 1385; (*c*) F. Tuna, L. Parton, Y. Journaux, M. Andruh, W. Plass and J.-C. Trombe, *J. Chem. Soc., Dalton Trans.*, 1999, 539; (*d*) M. Rodríguez, A. Llobet, M. Corbella, A. E. Martell and J. Reibenspies, *Inorg. Chem.*, 1999, **38**, 2328 and references cited therein; (*e*) H. Grove, J. Sletten, M. Julve and F. Lloret, *J. Chem. Soc., Dalton Trans.*, 2001, 1029.

8 (*a*) P. Alemany and S. Alvarez, *Chem. Mater.*, 1990, **2**, 723; (*b*) R. Cortes, L. Lezama, J. I. Ruiz de Larramendi, G. Maddariaga, J. L. Mesa, F. J. Zuniga and T. Rojo, *Inorg. Chem.*, 1995, **34**,

778; (*c*) M. Hernández-Molina, J. González-Platas, C. Ruiz-Perez, F. Lloret and M. Julve, *Inorg. Chim. Acta*, 1999, **284**, 258; (*d*) H. Grove, J. Sletten, M. Julve and F. Lloret, *J. Chem. Soc., Dalton Trans.*, 2001, 2487 and references therein.
9 (*a*) Y. Kani, S. Ohba, S. Ito and Y. Nishida, *Acta Crystallogr., Sect. C*, 2000, **56**, e195; (*b*) P. S. Donnelly, J. M. Harrowfield, B. W. Skelton and A. H. White, *Inorg. Chem.*, 2000, **39**, 5817.
10 (*a*) H. L. Zhu, L. M. Zheng, D. G. Fu, P. Huang, W. M. Bu and W. X. Tang, *Inorg. Chim. Acta*, 1999, **287**, 52; (*b*) S. Descurtins, H. Schmalle, P. Schneuwly, L. M. Zheng, J. Ensling and A. Hauser, *Inorg. Chem.*, 1995, **34**, 5501.
11 (*a*) X. H. Bu, M. Du, Z. L. Shang, R. H. Zhang, D. Z. Liao, M. Shionoya and T. Clifford, *Inorg. Chem.*, 2000, **39**, 4190; (*b*) X. H. Bu, M. Du, L. Zhang, Z. L. Shang, R. H. Zhang and M. Shionoya, *J. Chem. Soc., Dalton Trans.*, 2001, 729; (*c*) X. H. Bu, M. Du, Z. L. Shang, L. Zhang, Q. H. Zhao, R. H. Zhang and M. Shionoya, *Eur. J. Inorg. Chem.*, 2001, 1551; (*d*) X. H. Bu, M. Du, L. Zhang, D. Z. Liao, J. K. Tang, R. H. Zhang and M. Shionoya, *J. Chem. Soc., Dalton Trans.*, 2001, 593; (*e*) M. Du, X. H. Bu, G. C. Wang, Y. M. Guo and R. H. Zhang, *Inorg. Chim Acta*, 2001, **320**, 192; (*f*) M. Du, Y. M. Guo, X. H. Bu, J. Ribas and M. Monfort, *New J. Chem.*, 2002, **26**, 645.
12 (*a*) W. K. Musker *Coord. Chem. Rev.*, 1992, **117**, 133; (*b*) C. A. Grapperhaus and M. Y. Darensbourg, *Acc. Chem. Res.*, 1998, **31**, 451 and references cited therein.
13 R. G. Jones *J. Am. Chem. Soc.*, 1949, **71**, 383.
14 (*a*) A. W. Addison, T. N. Rao, J. Reedijk, J. V. Rijn and G. C. Verschoor, *J. Chem. Soc., Dalton Trans.*, 1984, 1349; (*b*) C. O'Sullivan, G. Murphy, B. Murphy and B. Hathaway, *J. Chem. Soc., Dalton Trans.*, 1999, 1835.
15 G. A. McLachlan, G. D. Fallon, R. E. Martin and L. Spiccia, *Inorg. Chem.*, 1995, **34**, 254.
16 S. J. Brudenell, L. Spiccia and E. R. T. Tiekink, *Inorg. Chem.*, 1996, **35**, 1974.
17 R. Lucas, S. Liu and L. K. Thompson, *Inorg. Chem.*, 1990, **29**, 85.
18 B. Bleaney and K. D. Bowers, *Proc. R. Soc. London, Ser. A.*, 1952, **214**, 451.
19 O. Kahn, *Molecular Magnetism*, VCH Publishers, New York, 1993.
20 This magnetic program uses the Hamiltonian $\boldsymbol{H} = -J\mathbf{S}_1\mathbf{S}_2$ by diagonalization of the matrices and was kindly supplied by the authors Dr Vassilis Tangouris, University of Patras, and Dr Dante Gatteschi, University of Firenze.
21 (*a*) A. M. Atria, A. Vega, M. Contreras, J. Valenzuela and E. Spodine, *Inorg. Chem.*, 1999, **38**, 5681; (*b*) C. R. Lucas and S. Liu, *Inorg. Chem.*, 1997, **36**, 4336.
22 J. L. Chou, J. P. Chyn, F. L. Urbach and D. F. Gervasio, *Polyhedron*, 2000, **19**, 2215.